ISSN 1070-3284, Russian Journal of Coordination Chemistry, 2021, Vol. 47, No. 1, pp. 95–104. © Pleiades Publishing, Ltd., 2021.

Synthesis, Crystal Structures of Gadolinium(III) and Erbium(III) Complexes Derived from Pyridine-2,6-Dicarboxylic Acid and Fluorescent Sensing of Picric Acid

S. Sharif[a], *, S. Zaheer[a], M. W. Mumtaz[b], O. Sahin[c], S. Ahmad[d], S. Zulfiqar[a], A. Adnan[a], and I. U. Khan[e]

[a] *Materials Chemistry Laboratory, Department of Chemistry, Government College University, Lahore, 54000 Pakistan*
[b] *Department of Chemistry, University of Gujrat, Gujrat, 50700 Pakistan*
[c] *Scientific and Technological Research Application and Research Center, Sinop University, Sinop, 57000 Turkey*
[d] *Department of Chemistry, College of Sciences and Humanities, Prince Sattam bin Abdulaziz University, Al-Kharj, 11942 Saudi Arabia*
[e] *Department of Chemistry, University of Sialkot, Sialkot, 51040 Pakistan*
**e-mail: mssharif@gcu.edu.pk*

Received January 27, 2020; revised March 13, 2020; accepted March 22, 2020

Abstract—Two new complexes of gadolinium(III) and erbium(III) with pyridine-2,6-dicarboxylic acid (H_2Pydc),$\{Na_3[Gd(Pydc)_3]\cdot 2H_2O\}_n$ (**I**) and $[Er(HPydc)_3]\cdot 10H_2O$ (**II**), were prepared and their crystal structures were determined by X-ray crystallography (CIF files CCDC nos. 940633 (**I**) and 872068 (**II**)). The gadolinium atom in **I** is nine-coordinate (GdN_3O_6) and exhibits a tricapped trigonal prismatic geometry having 14 triangular faces. The Pydc ligand adopts chelating and, μ_3- and μ_5-bridging coordination modes. The 1D chains are further joined by Na atoms to generate a 3D coordination polymer. The structure is additionally stabilized by H-bonding. The Erbium polyhedron in **II** is also a tricapped trigonal prism (ErN_3O_6). The HPydc anions in **II** behave as tridentate chelating ligands. The complex molecules are connected to each other through hydrogen bonding interactions to form a three-dimensional network. Fluorescence titration experiments for complex **II** displayed highly sensitive fluorescence quenching efficiency of 98.3% against picric acid.

Keywords: gadolinium(III), erbium(III), pyridine-2,6-dicarboxylate, crystal structure, fluorescence quenching

DOI: 10.1134/S1070328420120076

INTRODUCTION

Lanthanide complexes of pyridine carboxylic acids, picolinic (pyridine-2-carboxylic), nicotinic (pyridine-3-carboxylic), isonicotinic (pyridine-4-carboxylic), and dipicolinic (pyridine-2,6-dicarboxylic) acids, have been widely studied [1–30] because of their luminescent [3, 7–15] and magnetic properties [1, 5, 18, 28–30]. Structural studies of these complexes demonstrate that the complexes of picolinic [1–3] and nicotinic acids [4–7] generally exist in the monomeric form, while those of isonicotinic acid [6–8] and pyridine-2,6-dicarboxylic acid (H_2Pydc) [10–30] are usually polymeric, e.g. $[Nd_3(\text{isonicotinate})_9(H_2O)_6]_n$ [6] and $(H_2Pip)_n[Nd_2(Pydc)_4(H_2O)_2]_n$ (H_2Pip = piperazine) [13]. Nicotinic and isonicotinic acids bind only through carboxylate oxygen atoms [4–8]. But in case of picolinic [1–3] and pyridine-2,6-dicarboxylic acids [10–30] the ring nitrogen atom is also able to coordinate to lanthanide ions. Thus, carboxylate ligands are unique in modern coordination chemistry. They allow to synthesize a variety of coordination compounds of divers structural types from mono [31, 32], oligonuclear [33–36], multinuclear and polymeric [37, 38], including metal organic frameworks [39–41] and supramolecular systems [42–45]. Because of the diversity of its coordination modes (Scheme 1), H_2Pydc is a flexible ligand [10–31, 46] and thus highly effective for the construction of lanthanide supramolecular structures. In some cases, the complexes are stabilized by the presence of suitable cations [13–18] including an example of gadolinium-sodium coordination polymer $Na[Gd(Pydc)_2(H_2O)_3]\cdot 4H_2O$ [14]. For the gadolinium complex sodium azide was used as a source of sodium metal. The azide ion did not participate in bonding although azide containing Gd(III) complexes are also known [47]. To explore further the structural features of such complexes, we report here the synthesis, crystal structures of two new

lanthanide complexes of H_2Pydc, $\{Na_3[Gd(Pydc)_3]\cdot 2H_2O\}_n$ (**I**) and $[Er(HPydc)_3]\cdot 10H_2O$ (**II**) and fluorescence quenching analysis for quantification of picric acid.

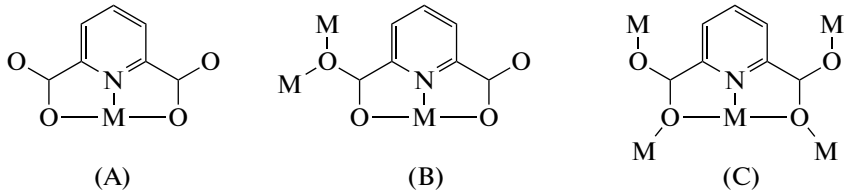

(A) (B) (C)

Scheme 1. Coordination modes of Pydc.

EXPERIMENTAL

Materials and measurements. Gadolinium nitrate, $Gd(NO_3)_3\cdot 6H_2O$ and erbium chloride ($ErCl_3\cdot 6H_2O$) were purchased from Alfa Aesar Company, USA and H_2Pydc was obtained from Merck Chemical Company, Germany. Emission and excitation spectra of complexes were measured using a Cary Eclipse bundle, Agilent fluorescence spectrophotometer. Elemental analysis was performed on the elemental analyzer, Vario Micro Cube, Elementar, Germany. FT-IR spectra were recorded on Bruker Tensor 27 FT-IR spectrometer with Diamond-ATR module over the range of 4000–400 cm^{-1}.

Synthesis of complex I. A mixture of H_2Pydc (134 mg, 0.80 mmol), 6 mL of water and 4 mL of methanol was refluxed at 120°C to dissolve the ligand followed by drop-wise addition of 5 mL aqueous solution of 181 mg (0.40 mmol) $Gd(NO_3)_3\cdot 6H_2O$ and 26 mg (0.4 mmol) sodium azide (NaN_3). The mixture was refluxed for 5 h. Off-white square-like crystals slowly grew in the filtered solution as solvent evaporated over three weeks. Crystals were recovered by filtration, rinsed with mixture of water and methanol (V: V = 80 : 20) and dried at room temperature (the yield was 65%).

For $C_{21}H_{13}N_3O_{14}Na_3Gd$ (M = 757.56)

Anal. calcd., %	C, 33.26	H, 1.72	N, 5.54
Found, %	C, 33.03	H, 2.05	N, 5.13

IR (ν, cm^{-1}): 3580–3235 ν(br, O–H), 3065 ν(C–H), 1585 ν(C=N), 1475 ν(C=C), 1622, 1418, 1387 ν(COO).

Synthesis of complex II. Erbium chloride hexahydrate (134 mg, 0.35 mmol) was added to a solution of H_2Pydc (84 mg, 0.50 mmol) in 15 mL water. The mixture was stirred under reflux for 4 h to attain a clear solution. Pink plate-like crystals grew slowly as the solvent evaporated over one month and recovered by filtration rinsed with water and dried at room temperature (the yield was 47%).

For $C_{21}H_{32}N_3O_{22}Er$ (M = 845.76)

Anal. calcd., %	C, 29.80	H, 3.78	N, 4.97
Found, %	C, 29.64	H, 3.58	N, 5.13

IR (ν, cm^{-1}): 3633–3240 ν(br.s, water O–H), 1624 ν_{asym}(C=O); 1432, 1385 ν_{sym}(C=O) [Pydc: 3063 (C–H), 1688, 1375 (COO), 1573 (C=N)].

X-ray structure determination. Suitable crystals of **I** and **II** were selected and data collection was performed at 296 K on a Bruker KAPA APEX II CCD diffractometer equipped with a four-circle goniometer and using MoK_α graphite mono-chromated radiation. The structures were solved by direct methods using SHELXS-97 and Crystals [48, 49] and refined by full-matrix least-squares methods on F^2 using WINGX [50]. All non-hydrogen atoms were refined with anisotropic parameters. Water H atoms were located in a difference map and refined subject to a DFIX restraint of O–H = 0.83(2) Å. All other H atoms were located from different maps and then treated as riding atoms with C–H distances of 0.93. Molecular diagrams were created using MERCURY [51]. Supramolecular analyses were performed and the diagrams prepared with the aid of PLATON [52]. Details of data collection and crystal structure determinations for complexes **I** and **II** are given in Table 1, the selected bond lengths and angles are listed in Table 2.

Crystallographic data for the structures of **I** and **II** have been deposited with the Cambridge Crystallographic Data Centre (CCDC nos. 940633 and 872068, respectively; e-mail: deposit@ccdc.cam.ac.uk or http://www.ccdc.cam.ac.uk).

Fluorescence study. The crystalline complex **II** was ground to powder and 1 mg of this powder was soaked in 10 mL of different solvents such as acetonitrile, dimethylformamide, methanol, tetrahydrofuran, ethanol, and distilled water followed by sonication for 30 min to get homogenous suspension prior to photoluminescence analysis. As shown in Fig. 1, maximum

Table 1. Crystallographic data and refinement details for complexes **I** and **II**

Parameter	Value	
Wavelength, Å	0.71073	0.71073
Crystal system	Monoclinic	Monoclinic
Space group	$C2/c$	$P2_1/c$
a, Å	17.9246(3)	17.9039(2)
b, Å	10.4778(2)	10.1620(2)
c, Å	18.3715(3)	18.6094(3)
β, deg	96.183(1)	112.260(1)
V, Å^3	3430.29(10)	3133.46(9)
Z	4	4
ρ_{calcd}, mg m^{-3}	1.467	1.793
μ, mm^{-1}	2.03	2.78
Measured reflections	14190	47833
Independent reflections	3359	6136
R_{int}	0.033	0.030
R_1 ($F^2 > 2\sigma(F^2)$)	0.048	0.023
wR_2 (F^2)	0.147	0.066
Goodness of fit on F^2	1.21	1.12
Largest difference peak and hole, e Å^{-3}	2.57/–1.17	1.39/–0.63

intensity was observed for MeCN-complex suspension.

A 5 mM stock solution of 2,4,6-trinitrophenol (TNP) was prepared in distilled water and diluted to different concentrations ranging from 0.2–1 mM. For the suspension of complex, 1 mg of **II** was added in 10 mL of acetonitrile sonicated for 30 min. Then, a solution of TNP (0.2–1 mM) was added into the above prepared suspension and a decrease in fluorescence intensity was measured. The quenching experiment was performed in triplicate to get consistent results.

RESULTS AND DISCUSSION

The infrared spectra of complexes **I** and **II** show broad bands with a maximum near 3400 cm^{-1}, assigned to the (O–H) stretch of water molecules. The bands due to the carboxylate asymmetric and symmetric stretches, ν_{as}(COO) and ν_s(COO), are sensitive to metal coordination as reported for other Pydc complexes [13, 14, 26]. The asymmetric mode ν_{as}(COO) of the free ligand at 1688 cm^{-1} shows a shift to a lower wave number on coordination (1622, 1624 cm^{-1}), indicating that the ligand is bound to the metal through the carboxylate oxygen. The symmetric mode ν_s(COO) is shifts to higher wave number on coordination when compared to the free ligand. The pyridine (C=N) and (C=C) stretches are observed at 1585 and 1475 cm^{-1} respectively.

The molecular structure of **I** along with the atom labeling is shown in Fig. 2a. The complex is polymeric with the asymmetric unit consisting of a half Gd^{3+} ion, one and a half each, Na^+ ions and Pydc ligands, and one non-coordinated water molecule. The Gd atom in **I** is nine-coordinated and exhibits a tricapped trigonal prism geometry attained by three nitrogen atoms (N(1), N(1)^i and N(2)) from three pyridine rings and

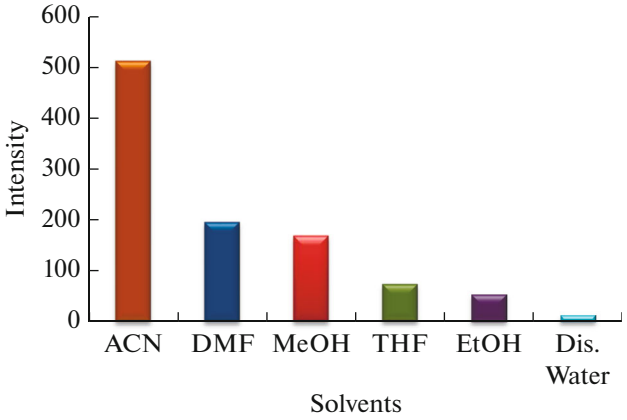

Fig. 1. Fluorescence intensity of 1 mg complex **II** in different solvents.

Table 2. Selected bond distances (Å) and angles (deg) for complexes **I** and **II***

Bond	*d*, Å	Bond	*d*, Å	Bond	*d*, Å
		I			
Gd(1)–N(1)	2.522(5)	Na(1)–O(6)^{ii}	2.821(5)	Na(1)–O(2)	2.816(5)
Gd(1)–O(1)	2.429(4)	Gd(1)–N(2)	2.515(6)	Na(2)–O(5)^{ii}	2.958(10)
Gd(1)–O(5)	2.443(4)	Gd(1)–O(3)	2.426(4)	Na(2)–O(2)	2.844(10)
		II			
Er(1)–O(2)	2.388(2)	Er(1)–O(5)	2.418(2)	Er(1)–N(1)	2.457(2)
Er(1)–O(30	2.388(2)	Er(1)–O(7)	2.375(2)	Er(1)–N(3)	2.458(3)
Er(1)–O(11)	2.411(2)	Er(1)–O(10)	2.393(2)	Er(1)–N(2)	2.470(3)
Angle	ω, deg	Angle	ω, deg	Angle	ω, deg
		I			
O(3)Gd(1)O(1)^{i}	76.37(15)	O(5)Gd(1)N(2)	63.93(9)	O(3)Gd(1)O(5)	147.58(15)
O(1)Gd(1)O(1)	149.3(2)	O(3)^{i}Gd(1)N(1)	74.49(15)	O(1)^{i}Gd(1)O(5)	88.99(15)
O(3)^{i}Gd(1)O(5)	77.53(15)	O(1)Gd(1)N(1)	63.89(14)	O(5)Gd(1)O(5)^{i}	127.86(19)
O(1)Gd(1)O(5)	77.58(14)	O(5)^{i}Gd(1)N(1)	73.09(14)	O(1)Gd(1)N(2)	74.65(10)
O(3)Gd(1)N(2)	135.61(11)	N(1)Gd(1)N(1)^{i}	120.8(2)	O(3)Gd(1)N(1)	64.00(15)
O(3)Gd(1)O(3)^{i}	88.8(2)	O(3)^{i}Gd(1)O(1)^{i}	127.87(14)	Gd(1)O(5)Na(2)	131.1(2)
		II			
N(1)Er(1)N(3)	120.52(8)	O(3)Er(1)N(2)	74.10(8)	O(3)Er(1)N(1)	134.44(8)
O(7)Er(1)O(10)	90.90(8)	O(3)Er(1)O(11)	89.48(8)	O(2)Er(1)O(5)	89.64(8)
O(2)Er(1)O(10)	147.80(8)	O(7)Er(1)N(1)	65.24(8)	O(10)Er(1)N(1)	73.93(8)
O(11)Er(1)N(1)	136.08(8)	O(10)Er(1)N(3)	134.81(8)	O(5)Er(1)N(2)	135.77(8)
O(11)Er(1)N(2)	64.52(8)	O(2)Er(1)N(2)	134.59(8)	O(2)Er(1)N(3)	64.91(8)
N(1)Er(1)N(2)	119.85(8)	N(1)Er(1)N(3)	120.52(8)	N(3)Er(1)N(2)	119.62(8)

* Symmetry codes: ^{i} $-x + 2, y, -z + 1/2$; ^{ii} $-x + 2, -y, -z$ for **I**.

six oxygen atoms (O(1), O(1)^{i}, O(3), O(3)^{i}, O(5), and O(5)^{i}) from six different carboxylic groups (^{i} $-x + 2, y, -z + 1/2$). The nitrogen atoms serve as the caps protruding through the prismatic side-faces (Fig. 3a). The GdN_3O_6 polyhedron is defined by 14 triangular faces. The Gd(III)–N bond distances are 2.515(6) and 2.522(5) Å, while the Gd(III)–O bond lengths are 2.426(4), 2.429(4) and 2.443(4) Å, which is typical in Gd(III) complexes with Pydc ligands [14, 19, 53–56]. The Na^+ ions exhibit two types of coordination environments. In the first type, the Na(1) atoms are coordinated by four oxygen atoms (O(2), O(2)^{iv}, O(6)^{ii}, and O(6)^{v}) from four different carboxylic groups (^{ii} $-x + 2, -y, -z$; ^{iv} $-x + 5/2, -y + 1/2, -z$; ^{v} $x + 1/2, y + 1/2, z$) possessing a square planer geometry (Fig. 3b). The Na(1)–O(2) and Na(1)–O(6)^{ii} bond lengths are 2.816(5) and 2.821(5) Å, respectively. In the second environment, the Na(2) atoms are two-coordinated by O(2) and O(5)^{ii} oxygen atoms as shown in Fig. 3c. The Na(2)–O(2) and Na(2) –O(5)^{ii} bond lengths are 2.844(10) and 2.958(10) Å, respectively. The Na–O bond lengths are longer than those found in other lanthanide complexes [2, 14, 18]. The structural parameters of **I** closely resemble to the analogous $Na_3[Ln(Pydc)_3] \cdot xH_2O$ complexes [16, 18].

In addition to one conventional mode (Scheme 1A) Pydc ligand adopts two types of coordination modes. In the first one, oxygen atoms of the carboxylate groups and the nitrogen atom of a pyridine ring form a chelate with one gadolinium atom. The second oxygen atom from one of the carboxylatebinds to two different sodium atoms. Thus, the Pydc ligand adopts both chelating and μ_3-bridging coordination modes to connect three metal atoms (Scheme 1B). In the second kind, oxygen atoms of the carboxylate groups in 2- and 6-position and the nitrogen atom of pyridine ring chelate one gadolinium atom, while each oxygen atom binds different sodium atoms. In this way, each Pydc ligand is bound to five metal ions. Therefore, the Pydc ligand adopts the chelating and μ_5-bridging modes (Scheme 1C). In Scheme 1C Pydc utilizes full coordination mode.

There are three sets of 1D chains found for **I**. In all three polymeric chains running parallel to the [100],

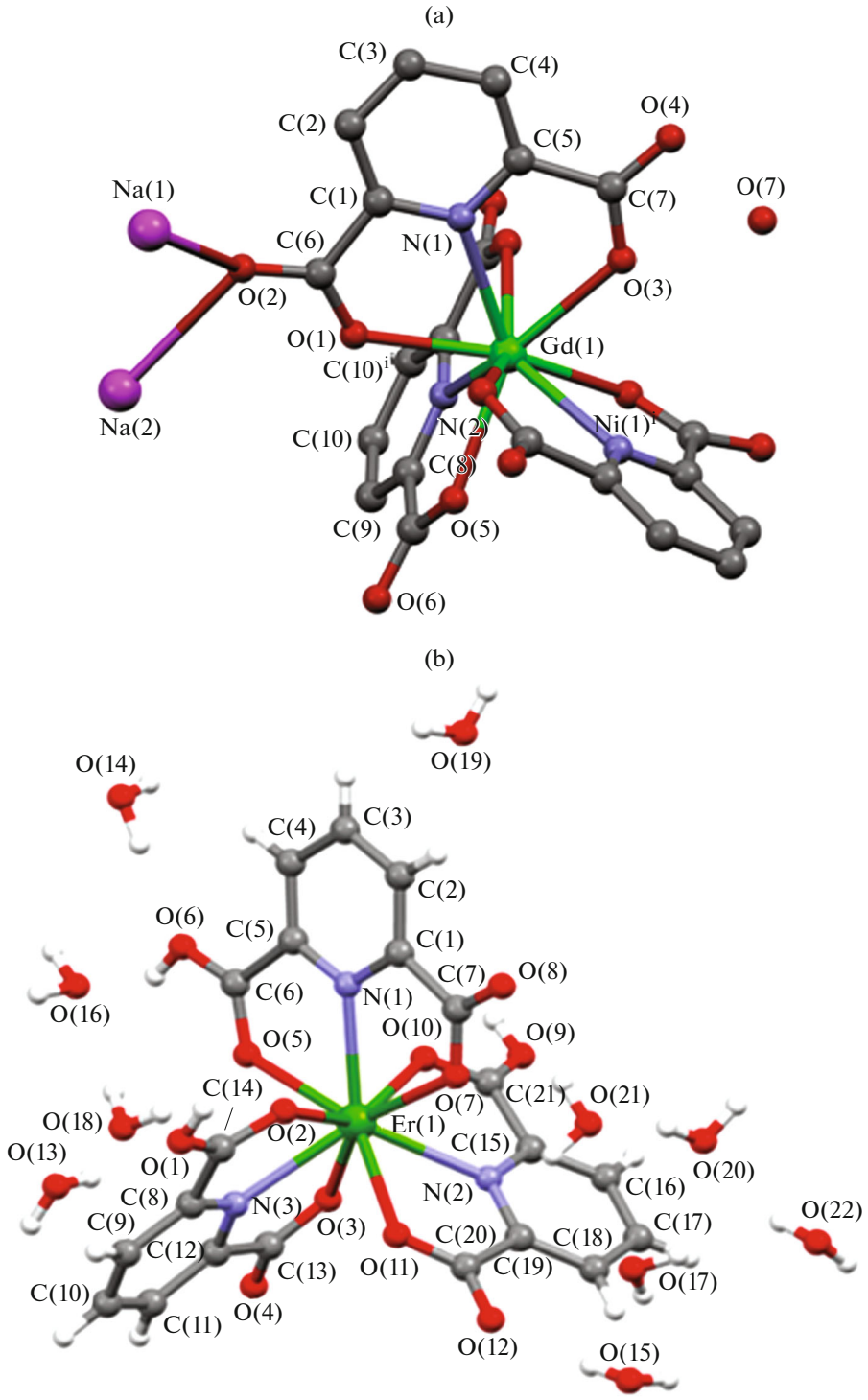

Fig. 2. The molecular structure of **I** (a) and **II** (b) showing the atomic numbering scheme. [i] $2 - x, y, 1/2 - z$ (a).

[010] and [001] direction, Gd^{3+} ions are coordinated by the oxygen atoms (O(1)) and (O(5)) of carboxylic groups from a symmetrically related Pydc anions with (O(2)) of Na(1) and Na(2) to generate an infinite 1D zigzag chain (Fig. 4a), grid-like 1D sheet (Fig. 4b) and straight 1D chain respectively (Fig. 4c). The Gd^{3+} ions are bridged by Pydc ligands and Na(2) atoms to generate 2D coordination polymer running parallel to the [001] direction, arranged in the form of rectangular grid-like 2D sheet with grid dimensions of 5.664 × 9.507 Å (defined by metal···metal distances) (Fig. 5a). The adjacent 2D coordination polymers are further

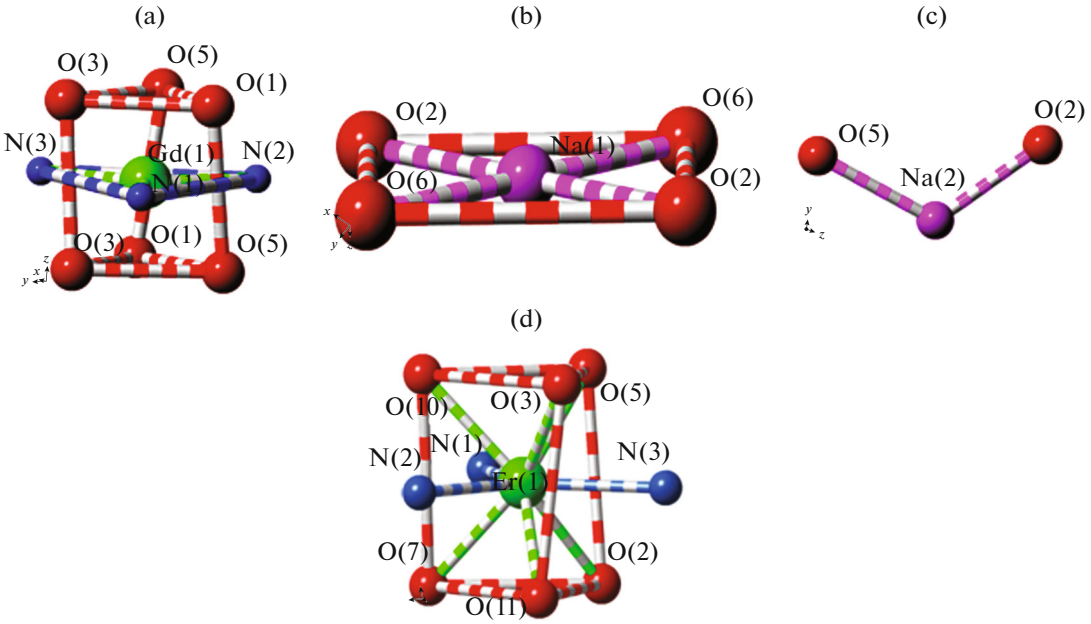

Fig. 3. Coordination geometry around Gd(III) (a), Na(I) (b), Na(II) (c) in **I** and Er(III) (d) in **II**.

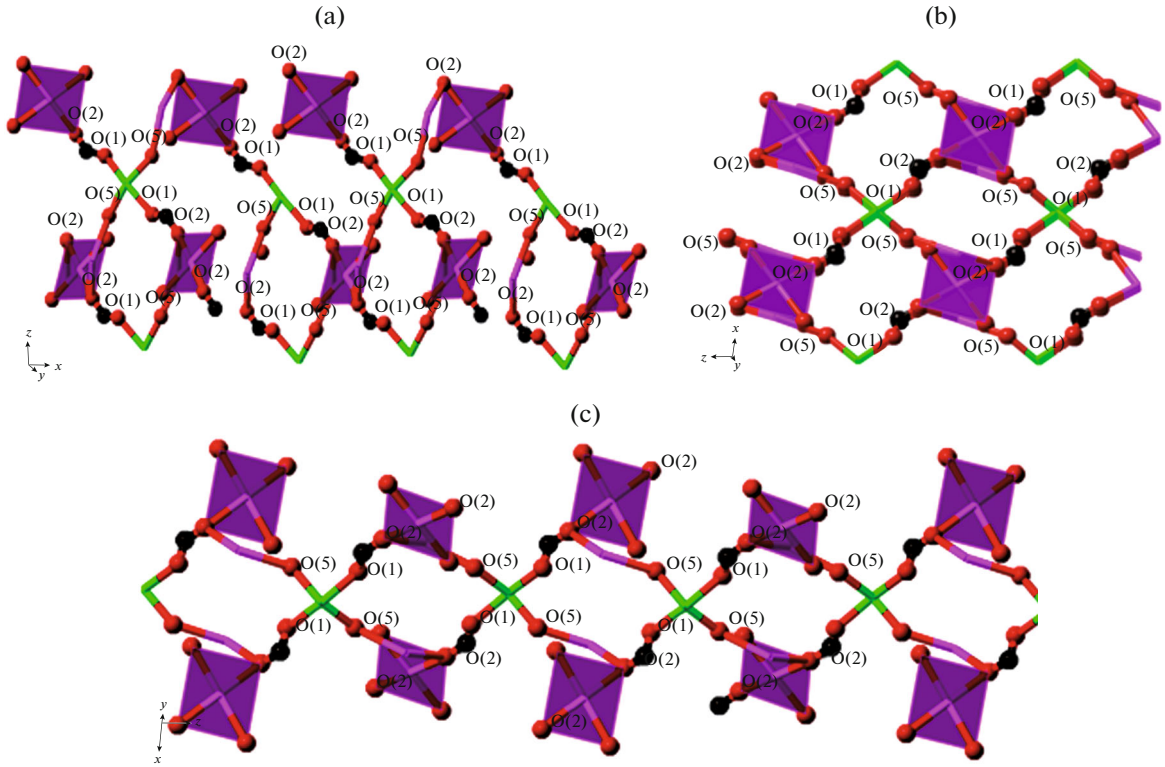

Fig. 4. 1D coordination polymer chain parallel to the [100] direction (a), 1D coordination polymer chain parallel to the [010] direction (b), 1D coordination polymer chain parallel to the [001] direction in **I** (c).

joined by Na(1) atoms, generating 3D coordination polymer. Adjacent Gd(III)···Gd(III) separations are 9.507 and 10.381 Å. The 3D coordination polymer is supported by O–H···O hydrogen bonds between water molecules and carboxylate oxygen atoms Table 3. The water molecules reside inside the 2D pores (Fig. 5b).

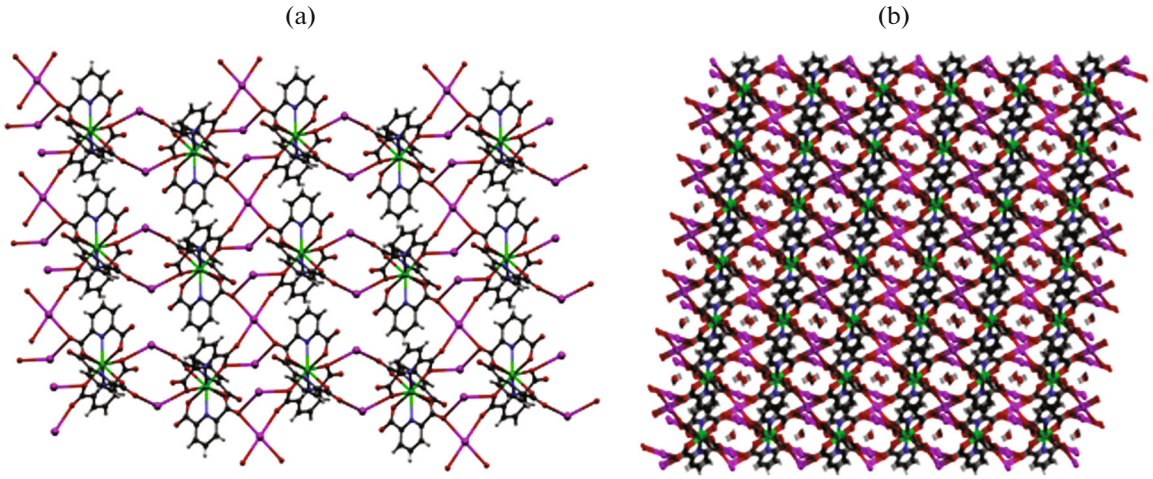

Fig. 5. An infinite 2D layer in **I** (a), an infinite 3D layer showing water molecules in pores (b).

The molecular structure of **II** is shown in Fig. 2b. The complex exists as discrete monomeric species comprising of and Er^{3+} ion coordinated by three mono-protonated HPydc ligands and ten non-coordinated water molecules. The Er^{3+} ion adopts a distorted tricapped trigonal prismatic geometry with the nitrogen atoms occupying the apical positions. The OErO and OErN bond angles range between 75.37(8)°–147.80(8)° and 64.52(8)°–136.08(8)°, respectively (Fig. 3d). The distortion in tricapped trigonal prismatic geometry is attributed to lower and upper distorted triangular faces with mean deviation of –3.446° and 7.244°, respectively, from regular triangular faces. Each HPydc ligand is coordinated to the Er(III) center in a conventional O,N,O'-tridentate fashion (Sheme 1A) [15–17, 55]. The carboxylate groups are essentially coplanar with their parent pyridine rings with maximum deviations of 0.0116(22) Å for N(1) atom, 0.0079(30) Å for C(17) atom and 0.0066(25) Å for C(12) atom, respectively. The bond distances of Er–O range between 2.375(2)–2.418(2) Å and that of Er–N range between 2.457(2)–2.470(3) Å, respectively. The Er–N and Er–O distances found in other structurally characterized Er(III)–Pydc complexes [15, 17]. The structure of complex **II** is very similar to the anionic Er(III)–Pydc complex $Na_3[Er(Pydc)_3] \cdot 13H_2O$ [15]. In the both complexes, Pydc (or HPydc) ligands coordinate only in the chelating form. On the other hand, in the polymeric $[Co(NH_3)_6][Er(Pydc)_3] \cdot 10H_2O$, they adopt the chelating as well as bridging modes [17].

The molecules of **II** are linked into sheets by a combination of O–H···O and C–H···O hydrogen bonds. Atom C(4) in the molecule at (*x, y, z*) acts as hydrogen-bond donor, via atom H(4), to atom $O(1)^{i}$, so forming a centrosymmetric $R_2^2(116)$ ring centered at (1/2, 1, 0). The hydrogen-bonds formed by H(9) to $O(8)^{ii}$ and H(11)–$O(9)^{ii}$ yield C(8) chains running parallel to the [010] direction. The combination of the C(8) chains along [010] generates a chain of edge-fused $R_2^2(12)$ rings (Fig. 6). Strong hydrogen bonds are observed between water molecules and oxygen atoms of carboxyl groups and water molecules, with the O···O distances range from 2.738(4) to 3.242(7) Å. Therefore, the packing diagram of **II** contains a 3D layer filled with crystal water molecules (Fig. 7). The geometrical parameters of the hydrogen bonds are given in Table 3. In coordination complexes **I** and **II**, Ln–O average bond lengths are decreasing from 2.426(4) to 2.375(2) Å and 2.515(6) to 2.457(2) Å for Ln–N with an increase in atomic number. The bond lengths from gadolinium to erbium are shortening by 2.10% for Ln–O and 2.30% for Ln–N, which can be ascribed to 20% decrease in ionic radii of lanthanide series from lanthanum 1.061 Å to lutetium 0.848 Å [57, 58].

Quenching efficiency was determined by gradual decrease in emission intensity of complex **II** from 512

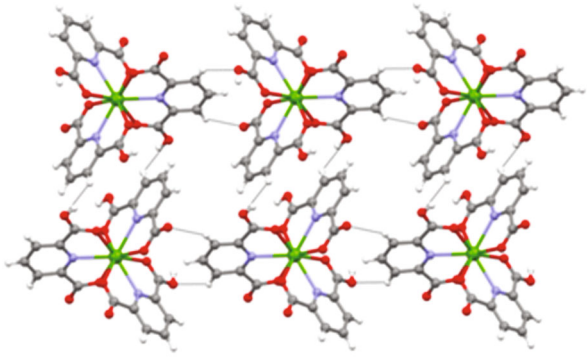

Fig. 6. Crystal structure of **II**, showing the formation of a chain along [010] generated by C–H···O hydrogen bonds.

Table 3. Geometric parameters of hydrogen bond for **I** and **II** *

D–H···A	Distance, Å			D–H···A, deg
	D–H	H···A	D···A	
		I		
O(7)–H(7A)···O(3)	0.93	1.97	2.794(13)	148
O(7)–H(7A)···O(4)	0.93	2.37	3.124(15)	139
C(4)–H(4)···O(2)^{vi}	0.93	2.45	3.239(9)	143
C(9)–H(9)···O(4)^{vii}	0.93	2.48	3.278(10)	144
		II		
O(1)–H(1)···O(14)^{i}	0.82	2.31	3.075(4)	155
O(6)–H(6)···O(16)	0.82	2.17	2.881(4)	146
O(13)–H(13*A*)···O(1)	0.85(2)	1.98(2)	2.811(4)	167(4)
O(13)–H(13*B*)···O(8)^{ii}	0.85(2)	2.10(3)	2.913(4)	163(4)
O(14)–H(14*A*)···O(6)	0.87(2)	1.96(2)	2.830(4)	173(5)
O(14)–H(14*B*)···O(18)^{iii}	0.87(2)	2.34(4)	3.054(5)	140(4)
O(14)–H(14*B*)···O(4)^{iii}	0.87(2)	2.55(4)	3.122(4)	124(4)
O(15)–H(15*A*)···O(12)	0.83(2)	1.93(2)	2.738(4)	164(5)
O(15)–H(15*B*)···O(4)^{iv}	0.82(2)	2.03(2)	2.850(4)	177(5)
O(16)–H(16*A*)···O(10)^{v}	0.84(2)	2.24(4)	2.912(4)	138(5)
O(17)–H(17*A*)···O(15)	0.84(2)	1.97(3)	2.756(5)	155(6)
O(17)–H(17*B*)···O(11)^{vi}	0.82(2)	2.06(2)	2.876(4)	179(7)
O(18)–H(18*A*···O(16)	0.82(2)	2.07(3)	2.857(5)	160(6)
O(18)–H(18*B*)···O(5)	0.82(2)	2.04(2)	2.846(4)	168(6)
O(19)–H(19*A*)···O(18)^{i}	0.82(2)	2.16(2)	2.974(6)	172(7)
O(19)–H(19*B*)···O(16)^{vii}	0.83(2)	2.08(3)	2.871(5)	159(7)
O(20)–H(20*A*)···O(17)^{vi}	0.83(2)	1.95(3)	2.760(6)	167(9)
O(20)–H(20*B*)···O(21)	0.82(2)	2.05(3)	2.845(8)	162(9)
O(21)–H(21*A*)···O(22)^{viii}	0.84(2)	2.47(4)	3.242(7)	153(6)
O(21)–H(21*B*)···O(8)	0.85(2)	2.02(2)	2.857(5)	173(8)
O(22)–H(22*A*)···O(20)	0.83(2)	2.09(3)	2.895(7)	163(7)
O(21)–H(21*B*)···O(7)	0.85(2)	2.54(7)	3.036(5)	118(6)
C(4)–H(4)···O(1)^{i}	0.93	2.55	3.232(4)	131
C(9)–H(9)···O(8)^{ii}	0.93	2.45	3.264(4)	147
C(11)–H(11)···O(9)^{ii}	0.93	2.59	3.338(5)	138

* Symmetry codes: ^{vi} $-x + 5/2, y + 1/2, -z + 1/2$; ^{vii} $-x + 2, y - 1, -z + 1/2$ (**I**). ^{i} $-x + 1, -y + 2, -z$; ^{ii} $x, y - 1, z$; ^{iii} $-x + 1, y + 1/2, -z + 1/2$; ^{iv} $-x, -y + 2, -z$; ^{v} $-x + 1, y - 1/2, -z + 1/2$; ^{vi} $-x, y + 1/2, -z - 1/2$; ^{vii} $x, -y + 5/2, z - 1/2$; ^{viii} $-x, y - 1/2, -z - 1/2$ (**II**).

to 174.1 a.u. as increasing concentration of picric acid as shown in Fig. 8. The decrease in intensity may be attributed to electron transfer from complex **II** to TNP molecule due to π–π interactions between aromatic ring of complex and TNP as well as polarizability of TNP [59, 60]. Quenching efficiency 98.3% of complex **II** against TNP was calculated by the following formula:

$$\%Q = 1 - \frac{I}{I_o} \times 100,$$

where, I is intensity of the complex after adding analyte and I_o is intensity of the complex before adding analyte.

Thus, we present in this report the crystal structures of a new hetero bimetallic polymeric gadolinium(III)–sodium(I) complex $\{Na_3[Gd(Pydc)_3]\cdot 2H_2O\}_n$ (**I**) and an erbium(III) monomeric complex $[Er(HPydc)_3]\cdot 10H_2O$ (**II**), obtained with pyridine-2,6-dicarboxylic acid. In both complexes, the central

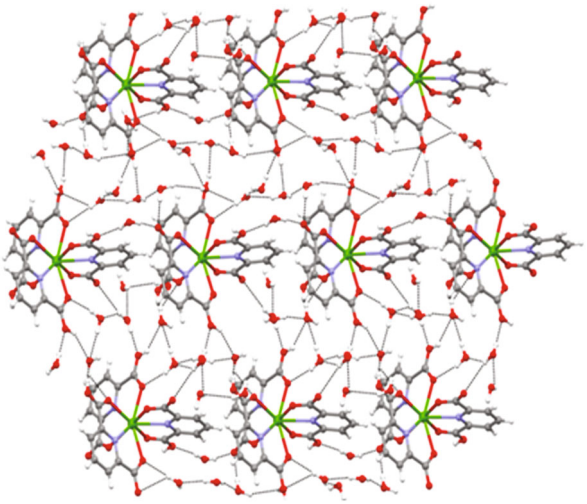

Fig. 7. View of 3D network of **II** showing solvent filled channels.

M^{3+} ions are nine-coordinated adopting a tricapped trigonal prism geometry. In case of **I**, sodium ions play an important role to assemble lanthanide and pyridine-2,6-dicarboxylate blocks to generate 3D coordination polymer. The complex **II** represents a rare example of such complexes containing only mono protonated Pydc ligand (HPydc). High quenching efficiency demonstrates the ability of complex **II** as an effective sensing material for picric acid.

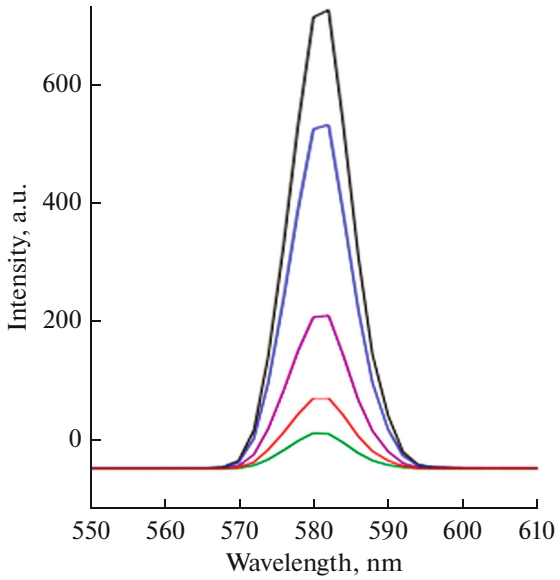

Fig. 8. Luminescence quenching of complex **II** dispersed in acetonitrile upon incremental addition of picric acid.

FUNDING

We gratefully acknowledge financial assistance from Higher Education Commission of Pakistan, HEC project no. 01-ISULL/09/GCUL/ACAD/HEC/2017/166 and Office of Research Innovation and Commercialization GC University, Lahore, ORIC project no. 108/ORIC/19.

REFERENCES

1. Girginova, P.-I., Pereira, L.C.J., Coutinho, J.-T., et al., *Dalton Trans.*, 2014, vol. 14, p. 1897.
2. Oh, Y., Kim, J.-Y., Kim, H.-J., et al., *Bull. Korean Chem. Soc.*, 2010, vol. 31, p. 1058.
3. Soares-Santos, P.C.R., Nogueira, H.I.S., Felix, V., et al., *Inorg. Chem. Commun.*, 2003, vol. 6, p. 1234.
4. Hussain, S., Khan, I.U., Elsegood, M.R.J., et al., *Polyhedron*, 2018, vol. 151, p. 452.
5. Hojnik, N., Kristl, M., Golobic, A., et al., *Eur. J. Chem.*, 2014, vol. 12, p. 220.
6. Sharma, S., Yawer, M., Kariem, M., et al., *Russ. J. Coord. Chem.*, 2015, vol. 41, p. 469.
7. Jia, G., Law, G.-L., Wong, K.-L., et al., *Inorg. Chem.*, 2008, vol. 47, p. 9431.
8. Han, L., Sun, X., Zhu, Y., et al., *J. Chem. Crystallogr.*, 2010, vol. 40, p. 579.
9. Xiang, S., Bao, D.-X., Wang, J., et al., *J. Lumin.*, 2017, vol. 186, p. 273.
10. Huang, Y.-G., Yuan, D.-Q., Gong, Y.-Q., et al., *J. Mol. Struct.*, 2008, vol. 872, p. 99.
11. Yang, L., Song, S., Shao, C., et al., *Synth. Met.*, 2011, vol. 161, p. 925.
12. Yang, L., Song, S., Shao, C., et al., *Synth. Met.*, 2011, vol. 161, p. 1500.
13. Ay, B., Yildiz, E., and Kani, I., *Polyhedron*, 2018, vol. 142, p. 1.
14. Zhu, T., Ikarashi, K., Ishigaki, T., et al., *Inorg. Chim. Acta*, 2009, vol. 362, p. 3407.
15. Reinhard, C. and Gudel, H.-U., *Inorg. Chem.*, 2002, vol. 41, p. 1048.
16. Albertsson, J., *Acta Chem. Scand.*, 1972, vol. 26, p. 985.
17. Brayshaw, P.A., Hall, A.K., Harrison, W.T., et al., *Eur. J. Inorg. Chem.*, 2005, p. 1127.
18. Hojnik, N., Kristl, M., Golobic, A., et al., *J. Mol. Struct.*, 2015, vol. 1079, p. 54.
19. Najafi, A., Mirzaei, M., Bauza, A., et al., *Inorg. Chem. Commun.*, 2017, vol. 83, p. 24.
20. Zhao, B., Yi, L., Dai, Y., et al., *Inorg. Chem.*, 2005, vol. 44, p. 911.
21. Ghosh, S.K. and Bharadwaj, P.K., *Inorg. Chem.*, 2004, vol. 43, p. 2293.
22. Duan, L., Li, Y., Liu, F., et al., *J. Mol. Struct.*, 2004, vol. 689, p. 269.
23. Prasad, T.K. and Rajasekharan, M.V., *Inorg. Chem.*, 2009, vol. 48, p. 11543.
24. Chuasaard, T., Panyarat, K., Rodlamul, P., et al., *Cryst. Growth Des.*, 2017, vol. 17, p. 1045.
25. Sharif, S., Sahin, O., Khan, I.-U., et al., *Crystals*, 2012, vol. 3, p. 1253.

26. Sharif, S., Khan, I.-U., Şahin, O., et al., *J. Inorg. Organomet. Polym. Mater.*, 2012, vol. 22, p. 1165.
27. Sharif, S., Şahin, O., Khan, B., and Khan, I.-U., *J. Coord. Chem.*, 2015, vol. 68, p. 2725.
28. Sharif, S., Khan, B., Sahin, O., and Khan, I.-U., *Russ. J. Coord. Chem.*, 2016, vol. 42, p. 56. https://doi.org/10.1134/S1070328416010048
29. Sharif, S., Khan, I.-U., and Sahin, O., *Z. Naturforsch., B*, vol. 74, p. 255.
30. Du, R.-Z., Wang, Y.-Y., Xie, Y.-Y., et al., *J. Mol. Struct.*, 2016, vol. 1108, p. 96.
31. Goldberg, A.E., Kiskin, M.A., Nikolaevskii, E., et al., *Russ. J. Coord. Chem.*, 2015, vol. 41, p. 182. https://doi.org/10.1134/S1070328415030021
32. Nikolaevskii, S.A., Evstifeev, I.S., Kiskin, M.A., et al., *Polyhedron*, 2018, vol. 152, p. 61.
33. Sidorov, A.A., Kiskin, M.A., Aleksandrov, G.G., et al., *Russ. J. Coord. Chem.*, 2016, vol. 42, p. 621. https://doi.org/10.1134/S1070328416100031
34. Goldberg, A., Kiskin, M., Shalygina, O., et al., *Chem. Asian J.*, 2015, vol. 11, p. 604. https://doi.org/10.1134/S1070328414070070
35. Nikolaevskii, S.A., Koshchienko, Y.V., Chernyshev, A.V., et al., *Russ. J. Coord. Chem.*, 2014, vol. 40, p. 468. https://doi.org/10.1134/S1070328414070070
36. Kiraev, S.R., Nikolaevskii, S.A., Kiskin, M.A., et al., *Inorg. Chim. Acta*, 2018, vol. 477, p. 15.
37. Kiskin, M.A. and Eremenko, I.L., *Russ. Chem. Rev.*, 2006, vol. 75, p. 559.
38. Bazhina, E.S., Gogoleva, N.V., Zorina-Tikhonova, E.N., et al., *J. Struct. Chem.*, 2019, vol. 60, p. 855.
39. Sapianik, A.A., Zorina-Tikhonova, E.N., Kiskin, M.A., et al., *Inorg. Chem.*, 2017, vol. 56, p. 1599.
40. Sapianik, A.A., Kiskin, M.A., Samsonenko, D.G., et al., *Polyhedron*, 2018, vol. 145, p. 147.
41. Sapianik, A.A., Lutsenko, I.A., Kiskin, M.A., et al., *Russ. Chem. Bull.*, 2016, vol. 65, p. 2601.
42. Adonin, S.A., Petrov, M.D., Novikov, A.S., et al., *J. Clust. Sci.*, 2019, vol. 30, p. 857.
43. Adonin, S.A., Novikov, A.S., Sokolov, M.N., et al., *Inorg. Chem. Commun.*, 2019, vol. 105, p. 221.
44. Adonin, S.A., Petrov, M.A., Abramov, P.A., et al., *Polyhedron*, 2019, vol. 171, p. 312.
45. Adonin, S.A., Bondarenko, M.A., Novikov, A.S., et al., *Cryst. Eng. Commun.*, 2019, vol. 21, p. 6666.
46. Tian, G., Rao, L., and Teat, S.-J., *Inorg.Chem.*, 2009, vol. 48, p. 10158.
47. Alexandropoulos, D.-I., Vignesh, K.-R., Dolinar, B.-S., and Dunbar, K.-R., *Polyhedron*, 2018, vol. 151, p. 255.
48. Sheldrick, G., *Acta. Crystallogr., Sect. A: Found. Crystallogr.*, 2008, vol. 64, p. 112.
49. Betteridge, P.-W., Carruthers, J.-R., Cooper, R-I., et al., *J. Appl. Cryst.*, 2003, vol. 36, p. 1487.
50. Farrugia, L.-J., *J. Appl. Cryst.*, 1999, vol. 32, p. 837.
51. Mercury, version 3.3, CCDC, ccdc.cam.ac.uk/products/mercury.
52. Spek, A.-L., *PLATON. A Multipurpose Crystallographic Tool*, Utrecht: Utrecht University, 2005.
53. Chen, Y., Chen, W., Ju, Z., et al., *Dalton Trans.*, 2013, vol. 42, p. 10495.
54. Elahi, S.M. and Rajasekharan, M.V., *Chem. Select.*, 2016, vol. 1, p. 6515.
55. Chen, Y., Gao, Q., Gao, D., et al., *J. Coord. Chem.*, 2013, vol. 66, p. 3829.
56. Gao, H.-L., Yi, L., Zhao, B., et al., *Inorg. Chem.*, 2006, vol. 45, p. 5980.
57. Zhao, B., Cheng, P., Dai, Y., et al., *Angew. Chem. Int. Ed.*, 2003, vol. 42, p. 934.
58. Zhao, B., Zhao, X.Q., Chen, Z., et al., *Cryst. Eng. Commun.*, 2008, vol. 10, p. 1144.
59. Barman, S., Garg, J.-A., Blacque, O., et al., *Chem. Commun.*, 2012, vol. 48, p. 11127.
60. Lv, C., Zhang, L., Li, J., et al., *Inorg. Chem. Commun.*, 2019, vol. 105, p. 240.